

Baseline evaluation of freshwater–saltwater interface in coastal aquifers of Badagry, south-western Nigeria

**Moroof O. Oloruntola, Adetayo
F. Folorunso, Olateju O. Bayewu, Ganiyu
O. Mosuro & Sadiq Adewale**

Applied Water Science

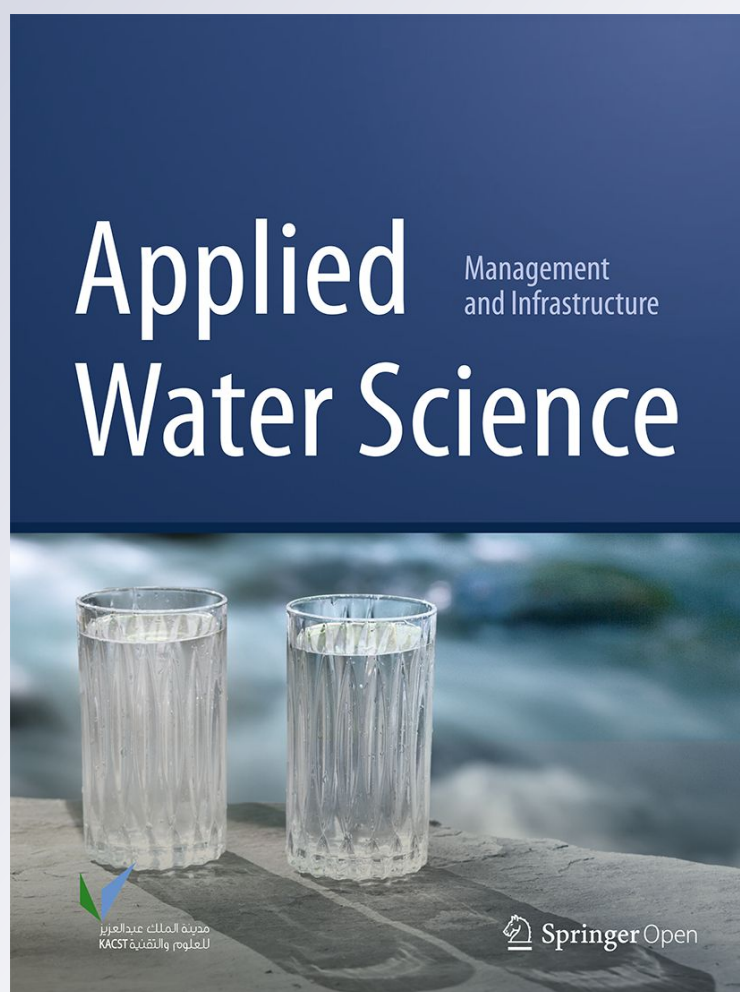
ISSN 2190-5487

Volume 9

Number 4

Appl Water Sci (2019) 9:1-14

DOI 10.1007/s13201-019-0957-1



Your article is published under the Creative Commons Attribution license which allows users to read, copy, distribute and make derivative works, as long as the author of the original work is cited. You may self-archive this article on your own website, an institutional repository or funder's repository and make it publicly available immediately.



Baseline evaluation of freshwater–saltwater interface in coastal aquifers of Badagry, south-western Nigeria

Moroof O. Oloruntola¹ · Adetayo F. Folorunso² · Olateju O. Bayewu³ · Ganiyu O. Mosuro³ · Sadiq Adewale¹

Received: 28 November 2017 / Accepted: 16 April 2019
© The Author(s) 2019

Abstract

This study focused on the evaluation of the baseline condition of saline water–groundwater interface in the coastal aquifers along Badagry, south-western Nigeria. Geologically, Badagry lies within the coastal sands and recent alluvium of the Dahomey Basin. Two-dimensional electrical resistivity tomography (2D-ERT) data along 15 survey lines were acquired in the study area, adopting the Wenner electrode arrays system with minimum spacing of 10 m. Ninety-one water samples were also collected, and their physical parameters were measured using hand-held devices. The (2D-ERT) data were processed and interpreted with the aid of DiProWin software. Sandy topmost layer, freshwater sand, brackish water sand and saline water sand were delineated from the study. Brackish water sand and freshwater sand layers were dominant in areas with high proximity to the Atlantic Ocean located in the south, which were not observed in the northern part of the mapped area. The study established the freshwater–saltwater interface at a depth of 10 m and above, in areas around the coast, while the interface occurs at depth greater than 50 m in areas 3–5 km from the coastal area. Observations from the pH and the TDS show that 87.3% of the samples are slightly acid, while less than 12.7% of them are slightly alkaline, while the TDS vary from 8 to 520 mg/l. The EC of the samples varies from 13 to 1140 $\mu\text{S}/\text{cm}$. All water samples are fresh groundwater, which confirms the occurrence of freshwater aquifer even in areas closer to the Atlantic Ocean.

Keywords Baseline · Freshwater · Saltwater · Interface · Coastal · Aquifers

Introduction

The probability of encountering freshwater in aquifers of coastal areas has been on the decline over time due to the influx of saline water from the sea towards land. Saline water intrusion is a phenomenon whereby saltwater displaces or mixes with fresh groundwater in coastal aquifers due to the density difference existing between waters of different salinities. Ideally, the groundwater flow pattern of fresh groundwater prevents saline water of the sea from encroaching coastal aquifers, hence creating an interface between freshwater and saltwater, which is maintained near the coast or

far below the land surface, known as zone of dispersion or transition zone (Fig. 1).

The problem of saltwater intrusion was recognized as early as 1854 on Long Island, New York (Back and Freeze 1983). The root cause of this problem is tied to geologic and anthropogenic factors, of which the anthropogenic factors are dominant. The ever-growing population of people who inhabit coastal areas has been a major reason for the increased rate of saline water intrusion, due to the increase in pumping rate in the quest for water use, which disrupts the ideal hydraulic flow pattern. Almost two-thirds of the world's population live within 400 km of the ocean shoreline, and just over half live within 200 km, an area only taking up 10% of the Earth's surface (Hinrichsen 2007). Most of these coastal regions rely on groundwater as their main source of freshwater for domestic, industrial and agricultural purposes.

There is a vital need to monitor the feasible risk of saline water intrusion of the coastal aquifers because, once saline water intrudes into coastal aquifer, it is extremely difficult to overcome and improve the management of the water

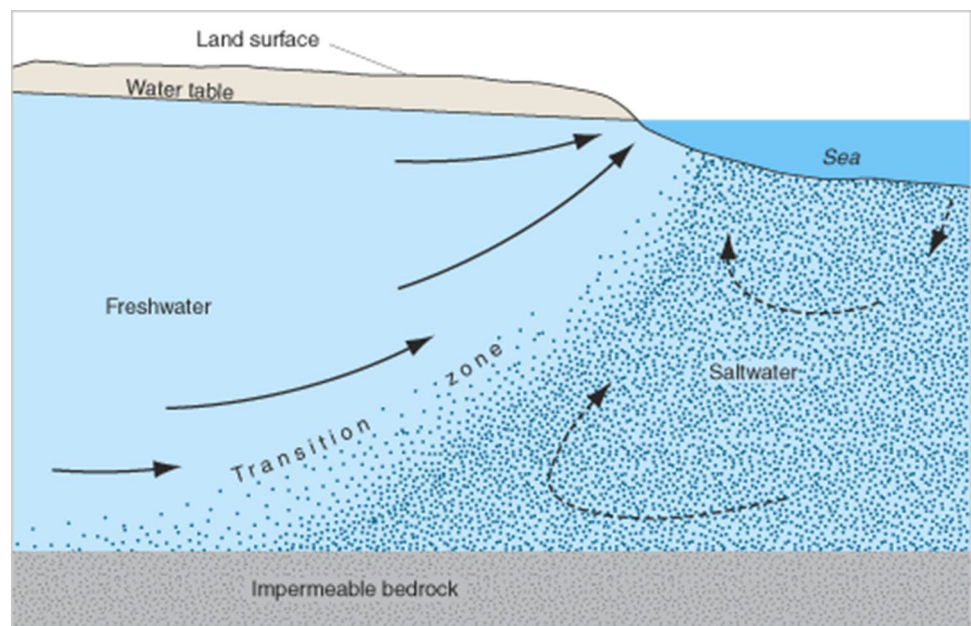
✉ Adetayo F. Folorunso
detayof@yahoo.com; affolorunso@futa.edu.ng

¹ Department of Geosciences, University of Lagos, Lagos, Nigeria

² Department of Marine Science and Technology, Federal University of Technology, Akure, Nigeria

³ Department of Earth Sciences, Olabisi Onabanjo University, Ago Iwoye, Nigeria

Fig. 1 Groundwater flow patterns and the freshwater–saltwater transition zone in an idealized coastal aquifer (Cooper 1964)



resources based on long-term strategy. Custodio (1987) concluded that less than 2% of seawater intrusion in the freshwater can diminish the water's potability. Frequently, when they occur, boreholes affected have to be abandoned and other water sources sought, which is often at high cost. The challenge of saline water contamination in coastal aquifers is driven by a violation of the delicate hydrogeological balance that exists between freshwater and seawater in coastal aquifers (Goldman and Kafri 2004). Saltwater intrusion occurs in virtually all coastal aquifers, where they are in hydraulic continuity with seawater. A number of brackish water zones in the subsurface are also produced due to mixing of saline water zones with freshwater ones (Choudhury et al. 2000). The need to understand problems associated with pressure on groundwater in coastal areas has been explained by Capizzi et al. (2010). These problems include seawater intrusion and the risks from agricultural, industrial and/or chemical contamination (Capizzi et al. 2010). Where seawater intrusion and groundwater contamination have occurred, groundwater can be restored through a number of reductions in rates of groundwater abstraction, relocation of abstraction works, increasing natural recharge, through favourable erosion control procedures, artificial recharge and simultaneous abstraction of saline water.

The Nigerian coastal areas are no exception to this phenomenon, of which places such as Burutu in Delta State (southern Nigeria) and Aiyetoro in Ondo State (south-western Nigeria) have no potable water source as the surface water is salty while drilled boreholes have yielded saline water (Oteri and Atolagbe 2003). Lagos State has carried out the most in terms of state-wide hydrogeological evaluation of its groundwater resources amongst all the

State and Federal Water Agencies in Nigeria (Kampsax-Kruger and Sshwed 1977; Coode Blizard Ltd. et al. 1996). The yearning desire to develop fresh groundwater in these regions has led to the study of groundwater occurrence using surface geophysical methods, well logs and other methods of study (Oteri 1988; Egbai and Efeyea 2013; Oladapo et al. 2014).

In many parts of the world, several studies have employed geophysical surveys around the coast for mapping freshwater–saline water interactions and effective groundwater management (Samsudin et al. 2002; Capizzi et al. 2010; Eloisa et al. 2012; Idowu et al. 2017). In some parts of the Lagos coastal area which extends east–west through the entire state, some attempts (essentially in eastern Lagos) have been made by using geophysical and/or geochemical techniques (Adepelumi et al. 2009; Ayolabi et al. 2013) to map saline water intrusion around coastal parts of Lagos.

The construction of the international highway and rail line between Lagos and Nigeria–Benin republic boundary has suddenly led to the geometric increase in human population and industrial activities in the hitherto less developed Badagry area, located in the western coast of Lagos. These activities have therefore led to increasing demand for potable water in a city with no municipal water facility in place. This, without doubt on the long run, will have effect on the freshwater–saltwater balance in this area. Oteri and Atolagbe (2003) affirmed that mapping of freshwater/saltwater interface(s) in most of the coastal aquifers in Nigeria is yet to be done. Therefore, this study is principally designed to provide baseline information on freshwater and saltwater horizons in the area and establish the physical character of shallow groundwater in Badagry area.

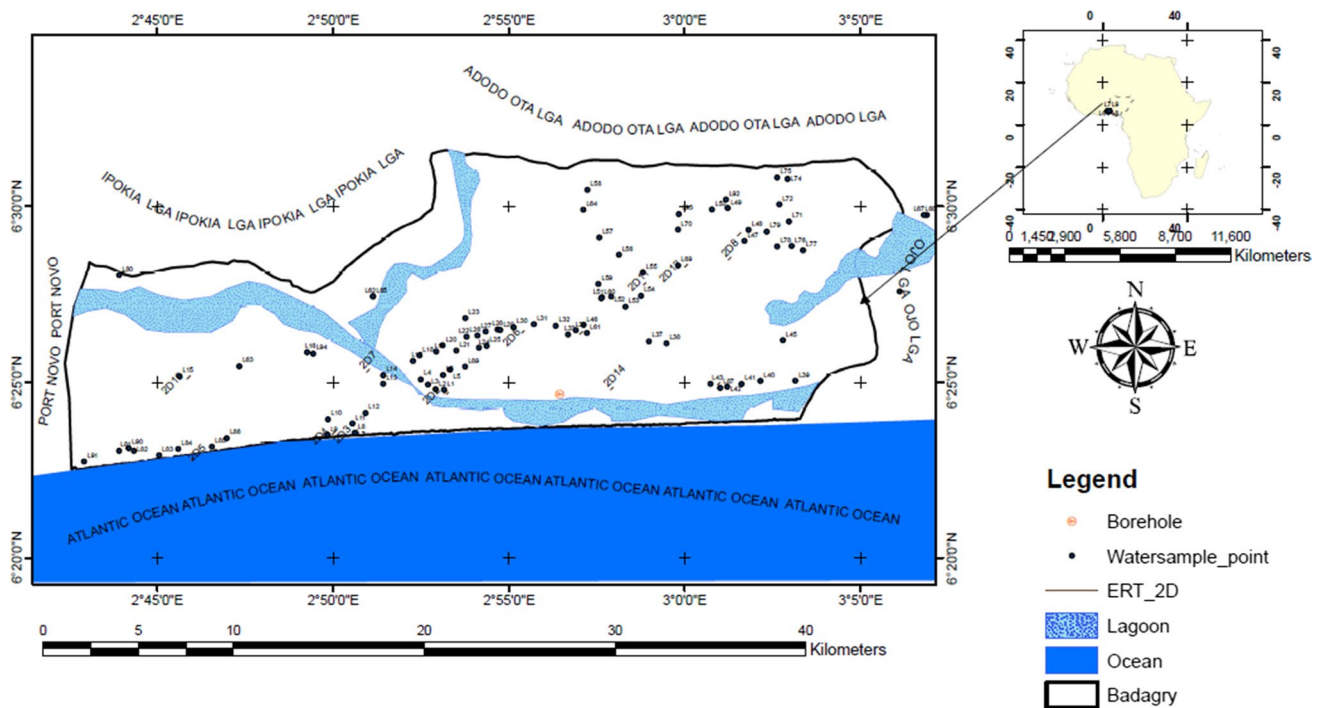


Fig. 2 Map of the area and survey distribution

Unlike most parts of coastal areas of Lagos, the area around the Badagry coast is still sparsely inhabited. However, reports from saltwater intrusion into the coastal aquifer have started to emanate in densely populated coastal areas of Lagos, such as the works of Adepelumi et al. (2009) and Ayolabi et al. (2013). Most of these areas have no baseline data to which the seawater intrusion studies were compared. This study therefore presents a great advantage as the basis to which environmental impact assessment of the area can be evaluated when the need will arise. The data from the baseline study will be domesticated in database for comparison with subsequent data to be acquired when the population is greatly appreciable.

The location and geology of the study area

Badagry is a coastal town and local government area (LGA) in Lagos State, south-western Nigeria (Fig. 2), and can be accessed via the Lagos-Badagry expressway. It lies within the tropical climate region, with an average temperature of 27.2 °C. March is the warmest month of the year with an average temperature of 28.9 °C. During August, the average temperature is 25.3 °C and hence represents the lowest average temperature of the whole year. The average temperature varies during the year by 3.6 °C. The average rainfall in the area is 1461 mm; January is the driest month with 19 mm of rain, while most precipitation

falls in June, with an average of 328 mm. This gives a difference of 309 mm of precipitation between the driest and the wettest months (Climate Data 2015). The area is drained by the Ologe Lagoon and water body of the Lac Nokoué (i.e. Lake Nokoué) which stretches down to Lagos from the Republic of Benin. Its vegetation is characterized by the swamp forest of coastal belt, which is a combination of mangrove forest and coastal vegetation developed under brackish conditions of the coastal areas and the swamp of the freshwater lagoons and estuaries.

The study area is underlain by sedimentary units of the Dahomey Basin as reported by various workers (Omatsola and Adegoke 1981; Nton 2001; Obaje 2009), who have mapped the area extensively. The exposed unit in the area is the coastal plain sands and recent alluvium, which are the youngest of the units constituting Dahomey Basin. The surface lithology in the area consists essentially of sands with the occurrence of clay intercalation in places. The sands are porous, and the occurrence of clay intercalations creates a multi-layered aquifer system.

The population of the Badagry area as at 2006 census was about 240,000 people. However, residential and industrial infrastructures are increasing significantly since the beginning of the construction of a 10-lane highway and rail line connecting the western coastal town to central Lagos.

Data and methods

Borehole log and geophysical data

Borehole log was obtained from GGS Geophysical Ltd., a consultant company, located in Badagry. The lithological description of samples obtained from the borehole with depth is a veritable control tool for the interpretation of the electrical resistivity survey.

Two-dimensional electrical resistivity tomography (2D-ERT) surveys were carried out in the study area using Campus Ohmega resistivity meter. Fifteen 2D-ERT surveys were acquired using the Wenner electrode configuration with progressive electrode spacing of $a = 10$ m, 20 m, 30 m, 40 m and 50 m (i.e. level $n = 5$), over a traverse length ranging from 120 to 210 m, depending on availability of space. The traverses were oriented perpendicular or near perpendicular to the Atlantic Ocean (towards south), in order to observe the variation in measured subsurface resistivity signature towards the Ocean as would be revealed by the resulting image of the Earth subsurface.

However, the electrodes were progressively moved along the traverse after each acquisition from the chosen first current electrode point to the last. Precaution measures were followed in order to ensure measurement of accurate readings and reduction in any interference noise. Resistance, R (Ω), measured was used to obtain the apparent resistivity (Ωm) which is the product of the resistance and was used for further data processing and interpretation.

We inverted the data using one of the flexible 2D-ERT inversion softwares called DIPPRO for window. It is a 2D forward modelling programme which calculates apparent resistivity pseudosection for 2D subsurface model by subdividing the subsurface into a number of rectangular cells where resistivities are varied to obtain the best fit with the observed data as described by Loke (2004). The programme's flexibility allows choosing the finite difference (FD) (Dey and Morrison 1979) or finite element (FE) (Silvester and Ferrari 1996) method to approximate the apparent resistivity values. The root-mean-square error (in %), which is a reflection of the differences between the observed and calculated data, is minimized to the barest minimum level to obtain an acceptable agreement (Loke and Baker 1996), which in this case is 0.5 rms was obtained. It then displays the resistivity model as resistivity variation with depth, where both the field and theoretical data pseudosections are displayed along with the inverted resistivity structure. (Sample is shown in Fig. 3.)

Physico-chemical data

Ninety-one water samples were collected randomly across the study location. The sampling was done in April 2015.

Physical parameters such as TDS, temperature, conductivity (using Hanna meter) and pH were measured and recorded in situ due to their unstable nature. Water samples were stored in accordance with the recommended preservation methods and holding period as given by Nigerian Standard for drinking water quality (NSDWQ) (2007). Depths to static water level in each of the wells were measured using Heron Instruments Inc.'s Dipper-T meter, which is calibrated to measure depth to static water level and produces/stops strong audible sound on contact with water.

Results and discussion

Description of borehole log

Borehole log (Fig. 4) of a well drilled to the depth of 168 m in the study area was obtained from a drilling company in order to serve as a lithological control for the interpretation of our resistivity data. The borehole revealed an area underlain predominantly by sands up to 21 m, with thin sandy clay layer (about 3 m thick) at a depth of about 21 m. A peat layer of about 0.2 m thick was encountered at a depth of about 50 m, underlain by sands of varying textures. The horizons penetrated by the borehole are within the coastal plain sands described by Jones and Hockey (1964), Okosun (1990) and Obaje (2009) as being composed essentially of alluvial deposits belonging to quaternary sediments.

Electrical resistivity tomography (ERT) survey

The ERT results are presented as 2D electrical resistivity structures in a colour scale of gradational blue to red, representing low to high resistivity values, respectively. This indicates the variation in the subsurface lithology and fluids content present beneath the surface. The tomography, in log scale, shows the lateral and vertical variation in resistivity to a depth of 50 m in the subsurface. The result of each electrical resistivity imaging is presented and discussed as follows.

Figure 5 shows the electrical resistivity imaging for the survey carried out over Traverse 2D-1 which is 130 m in length. It started from the coastline away from the water body. It reveals a decreasing resistivity values down from the surface (topsoil) indicating three geoelectric layers: a topmost sandy layer with resistivity of 151 Ωm , underlain by about 7-m-thick brackish-water-bearing sand with resistivity range of 20–51 Ωm , and this layer is underlain by saline-water-bearing sand of about 32 m thick with resistivity values less than 10 Ωm .

The resistivity imaging of Traverse 2D-2 is 200 m in length as shown in Fig. 6. This delineates a 5-m-thick sandy topmost layer with resistivity value of 92 Ωm , underlain by 3 m thickness of brackish-water-bearing sand

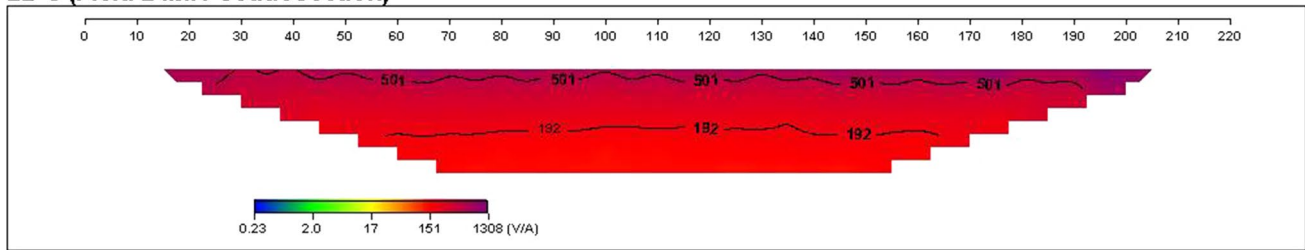
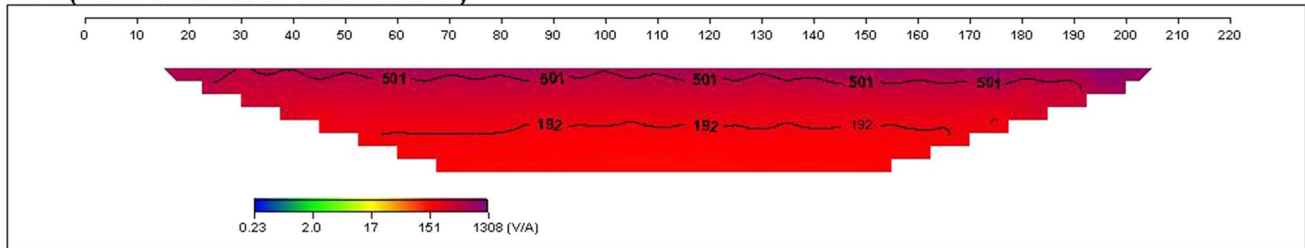
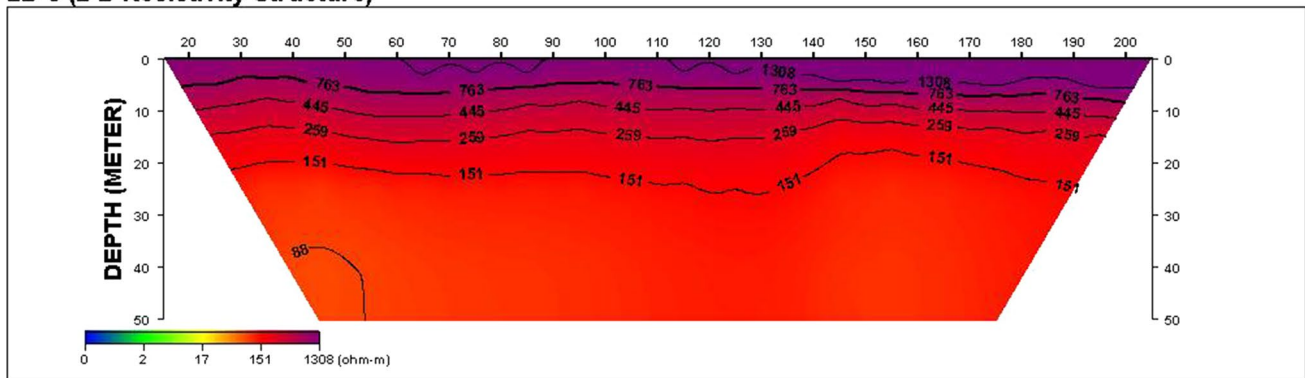
2D-8 (Field Data Pseudosection)**2D-8 (Theoretical Data Pseudosection)****2D-8 (2-D Resistivity Structure)**

Fig. 3 Representative samples of the inverted data showing the field and theoretical data pseudosections and the inverted 2D resistivity structure

with resistivity value of about $35 \Omega\text{m}$, and this is underlain by saline-water-bearing sand with resistivity value of $3.3 \Omega\text{m}$. The traverse also originates from the coastline into the shore.

Figure 7 depicts the resistivity imaging of Traverse 2D-3 survey established over a length of 200 m. It reveals a 5-m-thick sandy topmost layer ($381 \Omega\text{m}$), 7-m-thick freshwater-bearing aquifer with resistivity value of $111 \Omega\text{m}$ and saline-water-bearing sand with resistivity value of $2.7 \Omega\text{m}$. The resistivity model of the transverse is displayed to begin from the coastline into the shore for uniformity.

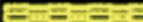

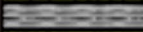
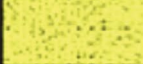











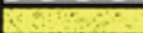








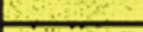


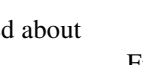
Resistivity model of Traverse 2D-4, about 50 m away from the coastline, is presented in Fig. 8. It was carried out over a 200-m-long line where a 7-m-thick sandy topmost layer with resistivity value of $1000 \Omega\text{m}$ was delineated. Underneath this layer was a 2-m-thick freshwater-bearing sandy aquifer with resistivity value of $310 \Omega\text{m}$ underlain by saline-water-bearing sand of $4.1 \Omega\text{m}$ resistivity value. Freshwater sand extends to a depth of up to 10 m above the

ground level. Beneath this depth, the water in the aquifer is essentially saline up to the delineated depth of 50 m.

A 7-m-thick sandy topmost layer with resistivity value of $381 \Omega\text{m}$, 4-m-thick freshwater-bearing sand with resistivity value of $111 \Omega\text{m}$ and saline-water-bearing sand with resistivity value of $9.4 \Omega\text{m}$ were delineated from the modelled electrical resistivity imaging (Fig. 9) over a 120 m long in Traverse 2D-5. The traverse is about 50 m closer to the coastline.

The modelled electrical resistivity imaging over a 140-m-long Traverse 2D-6 is shown in Fig. 10. This revealed an 8-m-thick sandy topmost layer with resistivity value of $674 \Omega\text{m}$ and a freshwater-bearing sandy layer with resistivity value of $179 \Omega\text{m}$ which is 7 m in thickness in the south-western end of the traverse and 42 m thick in the north-eastern end of the traverse, and this is underlain by brackish-water-bearing sand with resistivity value of $47 \Omega\text{m}$. This line located perpendicular to the sea contains freshwater sands up to the delineated depth of 50 m. There is absence of saline

Fig. 4 Borehole log of a well drilled through the coastal plain sands in the study area

DEPTH(M)	LITHOLOGY	DESCRIPTION	REMARKS
0 - 3		Fine grained clayey sand	Topsoil
3 - 18		Fine grained sand	Aquifer
18 - 21		Dark sandy clay	Confining layer
21 - 30		Fine grained sand	Aquifer
30 - 33		Coarse grained sand	
33 - 39		Sandy clay	Confining layer
39 - 42		Coarse grained sand	Aquifer
42 - 45		Sandy clay	Confining layer
45 - 51		Fine grained sand	Aquifer
51 - 57		Sandy clay	Confining layer
57 - 60		Fine grained sand	Aquifer
60 - 69		Coarse grained sand	
69 - 75		Fine grained sand	
75 - 96		Coarse grained sand	
96 - 99		Fine grained sand	
99-102		Sandy clay	Confining layer
102-105		Fine grained sand	Aquifer
105-108		Coarse grained sand	
108-111		Sandy clay	Confining layer
111-114		Fine grained sand	Aquifer
114-123		Sandy clay	Confining layer
123-126		Coarse grained sand	Aquifer
126-132		Fine grained sand	
132-138		Coarse-fine grained sand	
138-141		Dark peat	Fibrous/Organic
141-153		Coarse-fine grained sand	Aquifer
153-156		Fine grained sand	
156-168		Coarse-fine grained sand	

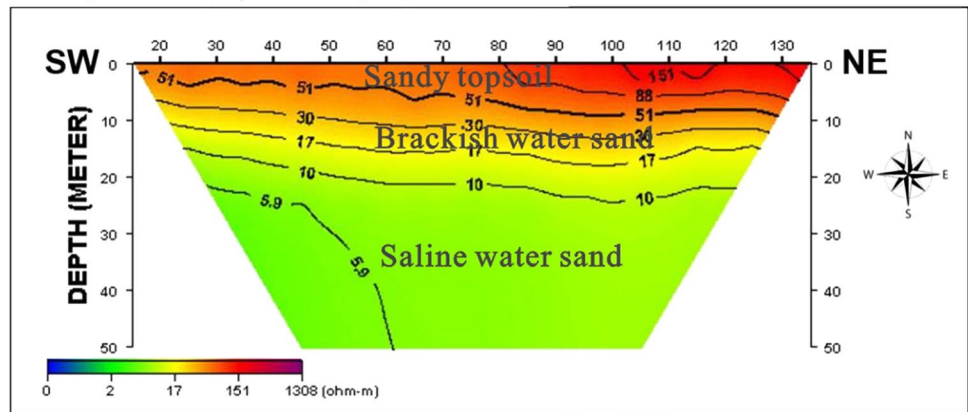
layer in the traverse because the traverse was located about 600 m away from the coastline.

The modelled resistivity imaging of the subsurface along a 210 m Traverse 2D-7 is shown in Fig. 11. Freshwater-bearing sand of 11 m thickness with resistivity value of 111 Ω m and saline-water-bearing sand with resistivity value of 9.4 Ω m were observed under the traverse. The profile is less than 200 m away from the coastline.

The resistivity imaging of Traverse 2D-8 is shown in Fig. 12, which was carried out over a length of 190 m very far away from the coastline (about 1 km away from the water body). It revealed a sandy topmost layer which is 10 m thick with a resistivity value of 763 Ω m, and this is underlain by freshwater-bearing sand layer with resistivity value of 151 Ω m. The saline-water-bearing sand and

Fig. 5 Resistivity imaging of Traverse 2D-1

2D-1 (2-D Resistivity Structure)



2D-2 (2-D Resistivity Structure)

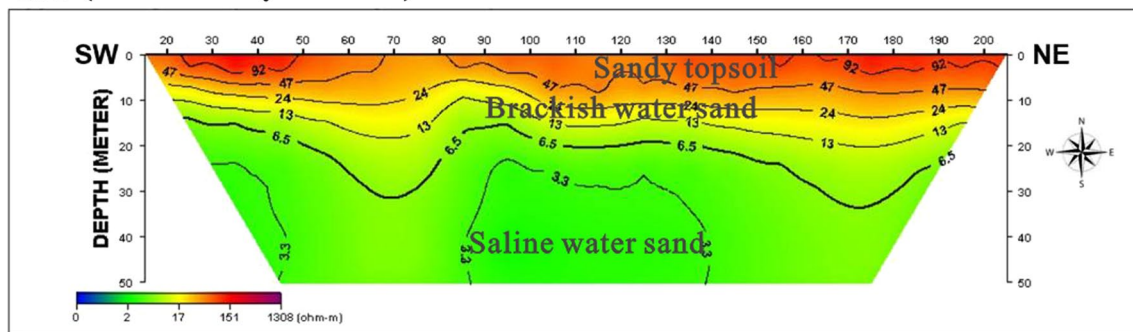


Fig. 6 Resistivity imaging of Traverse 2D-2

2D-3 (2-D Resistivity Structure)

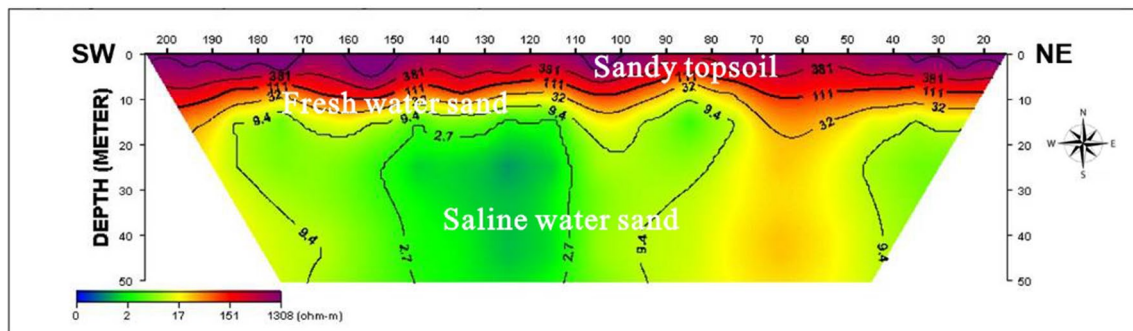


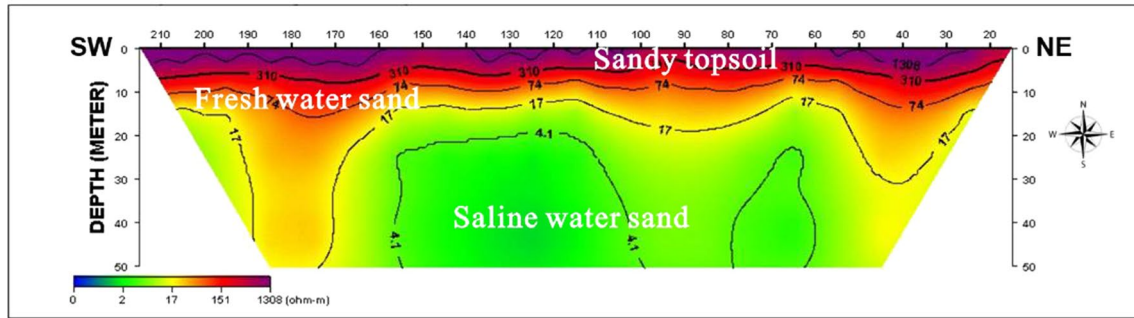
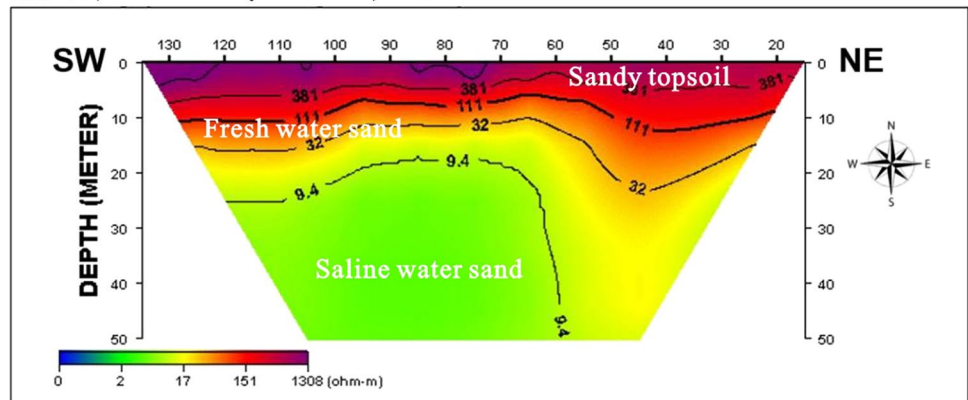
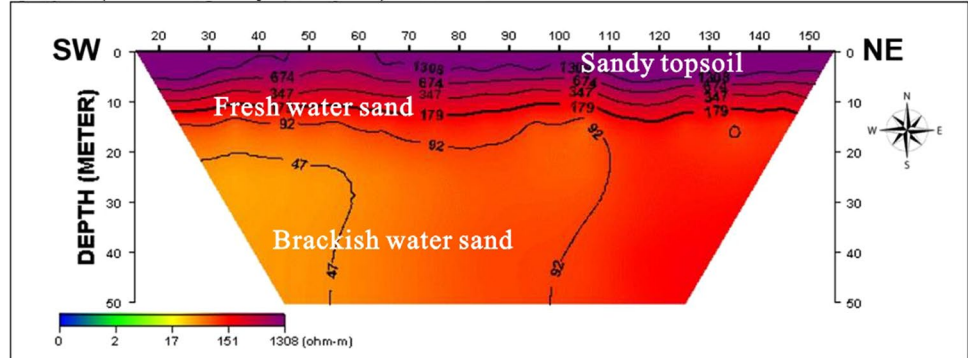
Fig. 7 Resistivity imaging of Traverse 2D-3

brackish-water-bearing sand are absent in this traverse owing to its distance to the coast.

The survey on Traverse 2D-9, 190 m long, reveals three layers with different fluid contents (Fig. 13). The topmost layer is composed of sand of about 10 m in thickness with resistivity value of 1308 Ω m, followed by a freshwater-bearing sand layer about 5 m thick in the south-western part of the traverse and 38 m thick in the north-eastern part of

the traverse. Below this is saline-water-bearing sandy layer towards the south-western part of the traverse with a resistivity value of 2.7 Ω m. The resistivity model shows how the saline layer under the traverse diminishes away from the coastline.

Figure 14 depicts the resistivity imaging of the acquired survey over a 210-m-long Traverse 2D-10. The resistivity imaging reveals an almost complete underlying saline

2D-4 (2-D Resistivity Structure)**Fig. 8** Resistivity imaging of Traverse 2D-4**Fig. 9** Resistivity imaging of Traverse 2D-5**2D-5 (2-D Resistivity Structure)****Fig. 10** Resistivity imaging of Traverse 2D-6**2D-6 (2-D Resistivity Structure)**

water sand layer except for the brackish water sand layer which is present at the shallow part of the resistivity traverse. The brackish-water-bearing sand is about 7 m thick in the south-western end of the traverse and 12 m thick in the north-eastern end of the traverse, with a resistivity value of 74 Ωm . The underlying saline-water-bearing sand has a resistivity value of 0.98 Ωm . The brackish water and saline water are evident in this traverse because of its nearness to the coastline.

The modelled resistivity imaging in Fig. 15, more than 1 km away from the coast, reveals the subsurface layers over Traverse 2D-11 which is 150 m long. The layers delineated are sandy topmost layer of about 10 m thick with resistivity value of 381 Ωm and underlying freshwater-bearing sand with resistivity value of 111 Ωm . The saline- and brackish-water-bearing horizons are absent in this traverse on account of its far distance from the coastline.

The resistivity imaging of the survey acquired along Traverse 2D-12, about 180 m long, is represented in Fig. 16.

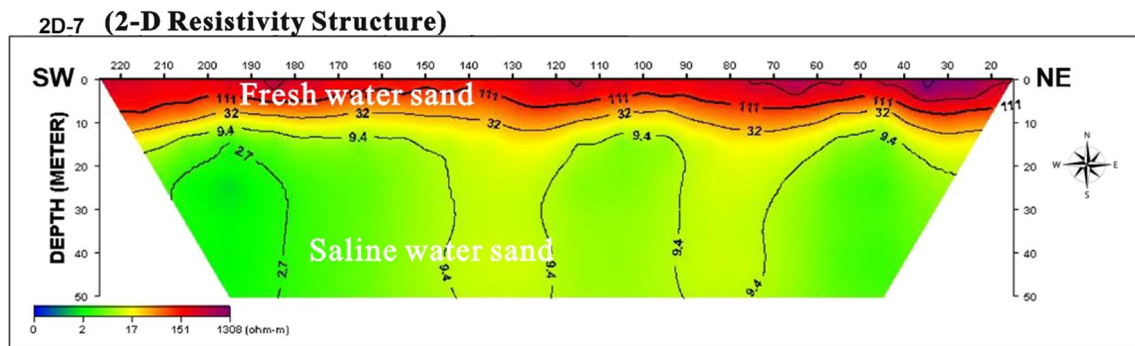


Fig. 11 Resistivity imaging of Traverse 2D-7

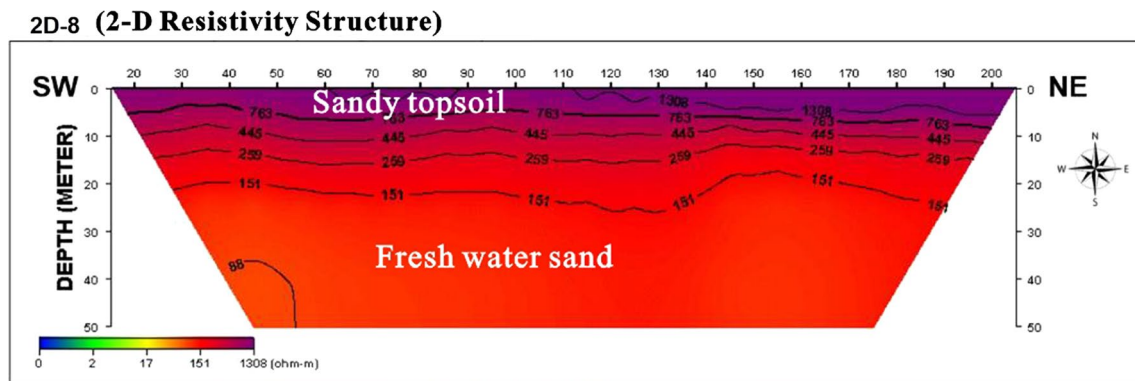


Fig. 12 Resistivity imaging of Traverse 2D-8

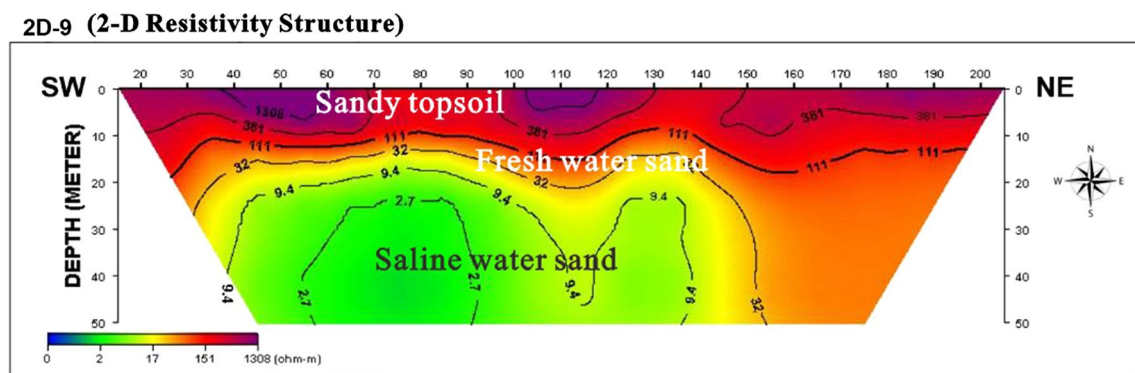


Fig. 13 Resistivity imaging of Traverse 2D-9

Similar geoelectric layers were delineated with varying degree of thickness. The topsoil is about 10 m in thickness with resistivity value of 597 Ωm , the freshwater layer with thickness range of 4–30 m from the south-western to the north-eastern end of the resistivity traverse, and a brackish-water-bearing sand layer with resistivity value of 26 Ωm . The saline layer is absent in this traverse as a result of its distance away from the coastline.

The condition of groundwater in the subsurface over a 200-m-long Traverse 2D-13 is shown in Fig. 17. The delineated layers are sandy topmost layer, which is about 10 m thick with a resistivity value of 414 Ωm , and freshwater-bearing sand with resistivity value of 131 Ωm . The saline- and brackish-water-bearing sandy layers are also absent in this traverse. This is also as a result of its distance away from the coastline (more than 1 km away).

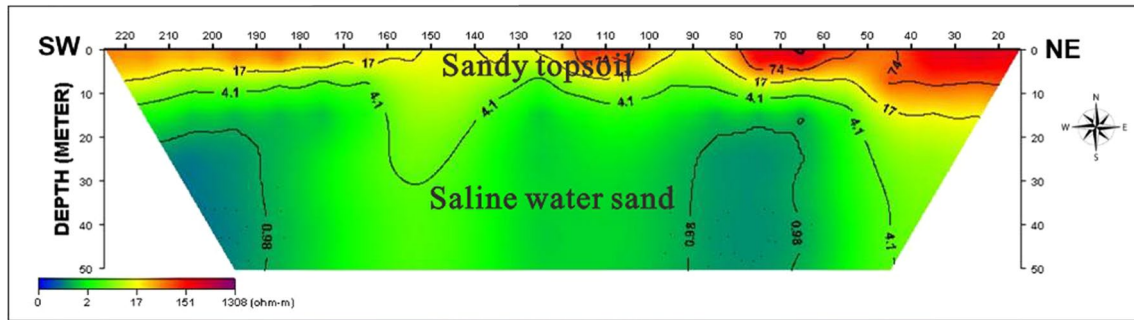
2D-10 (2-D Resistivity Structure)

Fig. 14 Resistivity imaging of Traverse 2D-10

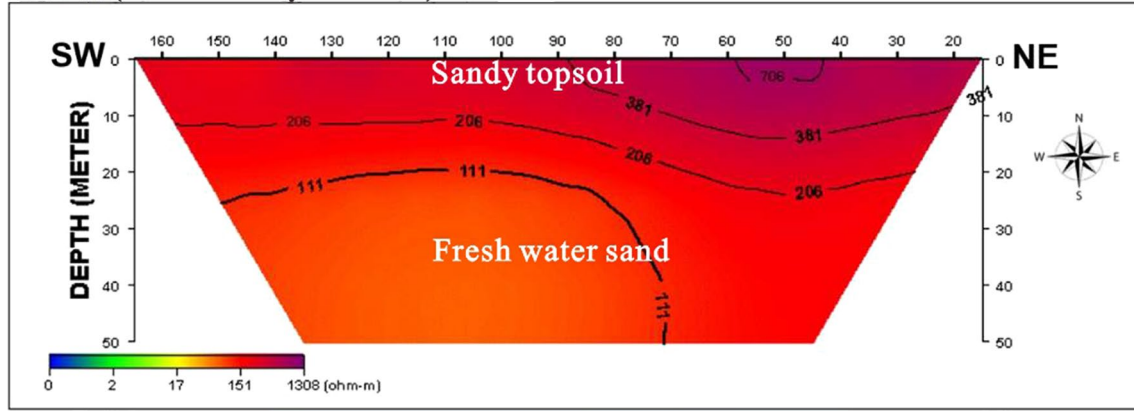
2D-11 (2-D Resistivity Structure)

Fig. 15 Resistivity imaging of Traverse 2D-11

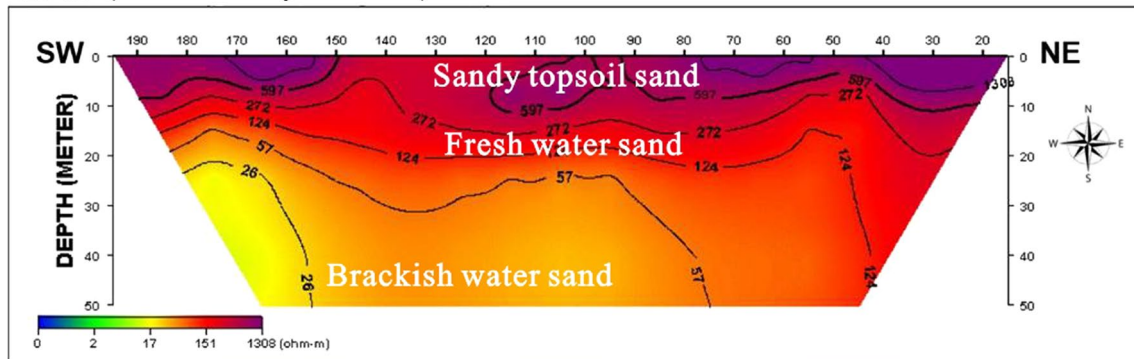
2D-12 (2-D Resistivity Structure)

Fig. 16 Resistivity imaging of Traverse 2D-12

Figure 18 shows the resistivity imaging acquired over a 160-m-long Traverse 2D-14. This delineates a 10-m-thick sandy topmost layer with resistivity value of 501 Ωm , brackish-water-bearing sand layer of 74 Ωm resistivity value and saline-water-bearing sand with resistivity value of 4.1 Ωm .

The resistivity imaging shown in Fig. 19 delineates a sandy topmost layer, freshwater sand and saline water sand. The resistivity imaging was acquired over a 150-m-long Traverse 2D-15. The sandy topmost layer is 10 m thick with resistivity of 1308 Ωm , the 10-m-thick

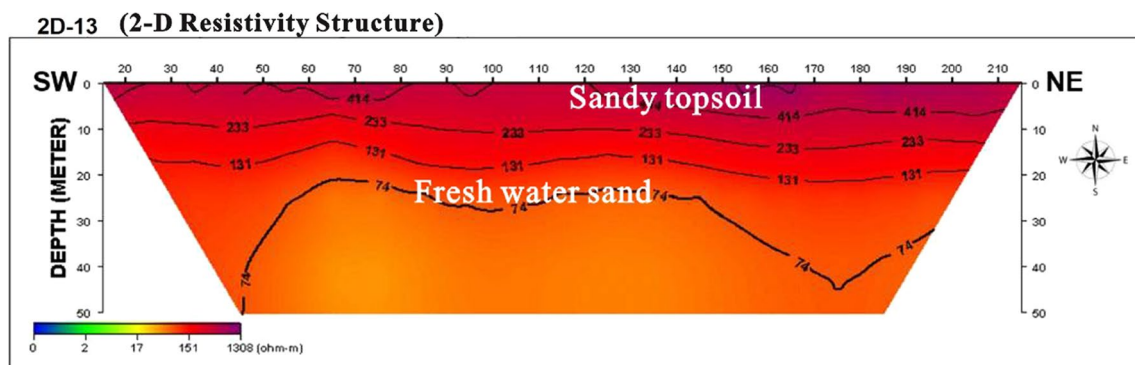


Fig. 17 Resistivity imaging of Traverse 2D-13

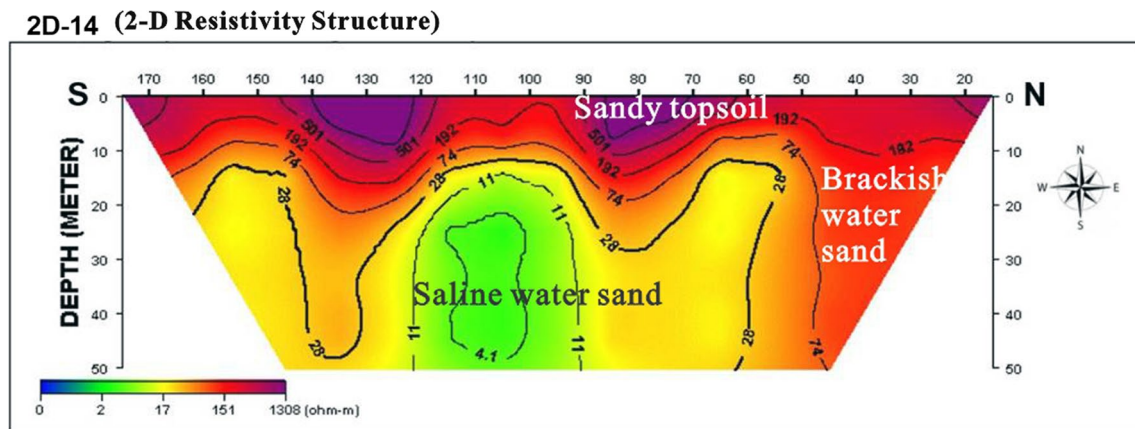


Fig. 18 Resistivity imaging of Traverse 2D-14

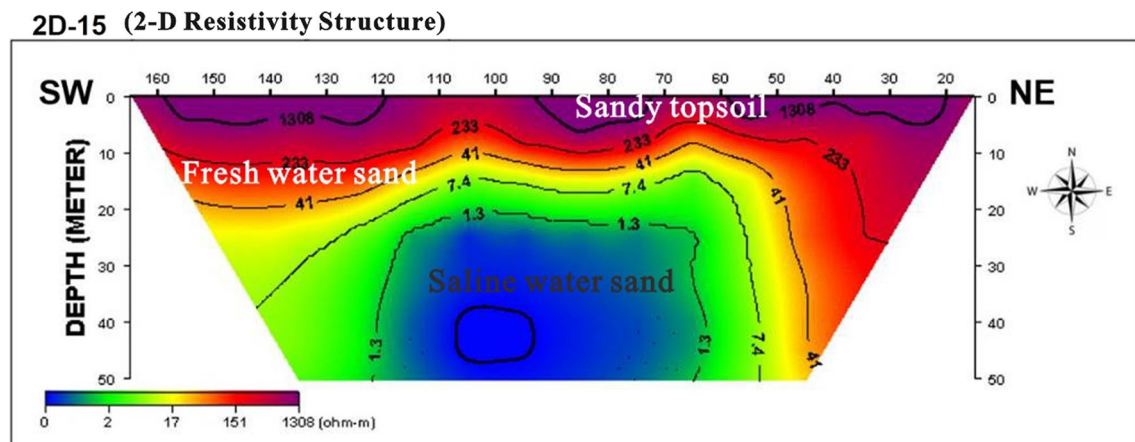


Fig. 19 Resistivity imaging of Traverse 2D-15

freshwater-bearing sand has resistivity value of 233 Ωm , and the underlying saline water sand has resistivity value of 1.3 Ωm .

Freshwater–saltwater interface in the study area

The depths to freshwater–saltwater interface in different areas around the study location are presented in Table 1. The

Table 1 Summary of estimated depths to saltwater

Profile no.	Delineated depth to saltwater sands (m)	Thickness of freshwater sands
2D-1	15	—
2D-2	10	—
2D-3	10	5
2D-4	10	5
2D-5	12	5
2D-6	Absence of saltwater sand	10
2D-7	10	1
2D-8	Absence of saltwater sand	20
2D-9	15	10
2D-10	8	Absent
2D-11	Absence of saltwater sand	20
2D-12	Absence of saltwater sand	12
2D-13	Absence of saltwater sand	19
2D-14	15	Absent
2D-15	16	9

depth varies from 8 to 16 m at distances of 165–4849 m from the ocean (measured north to south). The mapped depth to the interface is partly influenced by the distances of the 2D locations to the ocean (measured N–S) and various anthropogenic (human) activities along the coast. Unlike all coastal areas of Lagos State, municipal residential and commercial activities around the Badagry coast are extremely low with total absence of industrial activities, for now. Therefore, the freshwater–saltwater balance around the Badagry coast is still largely unaltered by abstraction of freshwater compared to the coast around Apapa and Lekki axes with fully developed residential and commercial properties. At distances greater than 5 km in the study area, the freshwater–saltwater interface occurs at depth greater than 50 m, the maximum depth delineated from the survey.

Summarily, the traverses that are closer to the ocean showed prominently the presence of saline- and

Table 2 Summary of the physico-chemical parameters of the groundwater in the study area

Parameters	Min	Max	Mean
TDS (ppm)	8	520	150
EC ($\mu\text{S}/\text{cm}$)	13	1140	317
pH	5	12.28	6.51
Temp ($^{\circ}\text{F}$)	24.3	32.6	29.2
Static water level (m)	0.3	14.45	2.88

brackish-water-bearing sandy layer with the evidence of low resistivity values at a depth greater than 10 m (less than 10 Ωm), while saline horizon occurs at a depth greater than 50 m in areas very far from the ocean.

Physico-chemical characteristics of groundwater in the study area

The summary of the physical parameters is presented in Table 2. Some of the parameters are presented as classed map to show their distribution relative to the coast. The pH has a range of 5–12.28. 87.3% of the samples are slightly acidic, while less than 12.7% of them are slightly alkaline, with pH value less than 8, except the only outlier (12.28) obtained very far from the coast (Fig. 20), from the deepest of the wells. The total dissolved solids (TDS) vary from 8 to 520 mg/l, having a mean of 150 mg/l (Fig. 21). All water samples are fresh groundwater based on Freeze and Cherry (1979) classification; this confirms the occurrence of freshwater aquifer even in area less than 100 metres to the Atlantic Ocean. The electrical conductivity (EC) of the samples (13–1140 $\mu\text{S}/\text{cm}$) also confirms the occurrence of freshwater in all the shallow wells (static water level of 0.3–14.45 m) in the area unlike in other coastal areas of Lagos where groundwater saline water intrusion has displaced freshwater in coastal aquifer with high proximity to the ocean (Adepelumi et al. 2009).

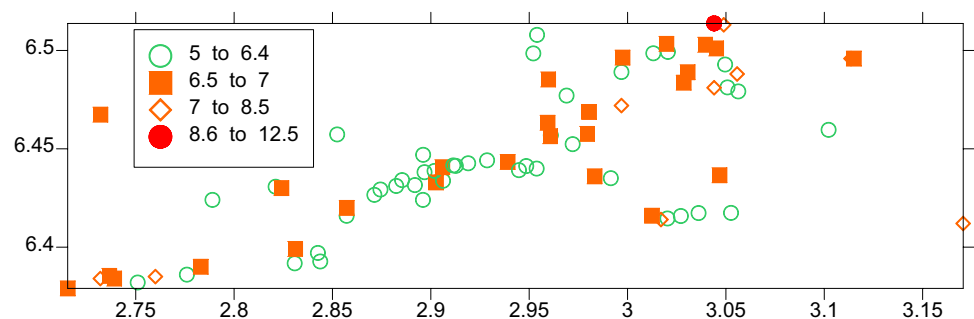
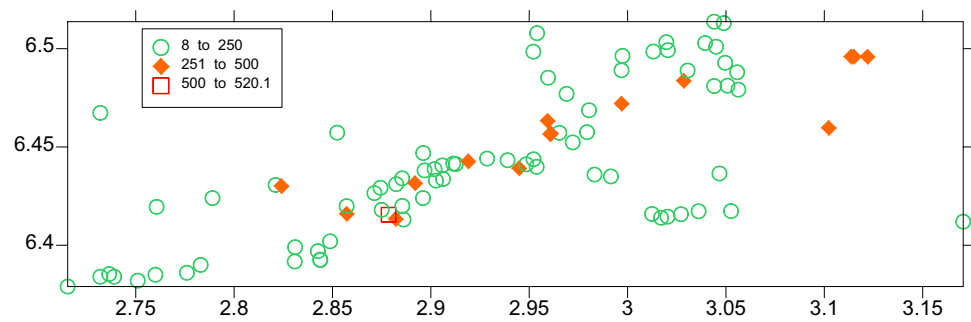
Fig. 20 Classed map of the pH in the study area

Fig. 21 Classed map of TDS

Conclusion

The 2D surveys and the physical parameters of groundwater have been used to establish the occurrence of freshwater aquifer in every part of the study area. In addition, the 2D survey established the freshwater–saline water interface at a depth greater than 10 m within the coastal subsurface with high proximity to the ocean and at an increasing depth farther away from the coast to a depth greater than 50 m. The geophysics data also revealed the presence of freshwater horizon beneath the study area, thereby indicating the contact between saline water and the freshwater layers. It was also noted that low developmental activities around the Badagry coast, resulting in low groundwater abstraction relative to the high precipitation which provides recharge, help to maintain the hydraulic balance for the freshwater–saltwater interface. Although with time, the balance will shift as population increases and the study will become a benchmark for the study of hydrological balance in the Badagry and its suburb.

Open Access This article is distributed under the terms of the Creative Commons Attribution 4.0 International License (<http://creativecommons.org/licenses/by/4.0/>), which permits unrestricted use, distribution, and reproduction in any medium, provided you give appropriate credit to the original author(s) and the source, provide a link to the Creative Commons license, and indicate if changes were made.

References

- Adepelumi AA, Ako BD, Ajayi TR, Afolabi O, Omotoso EJ (2009) Delineation of saltwater intrusion into the freshwater aquifer of Lekki Peninsula, Lagos, Nigeria. *J Environ Geol* 56(5):927–933
- Ayolabi EA, Folorunsho AF, Odukoya AM, Adeniran AE (2013) Mapping saline water intrusion into the coastal aquifer with geophysical and geochemical techniques: the University of Lagos campus case (Nigeria). *SpringerPlus* 2:433
- Back W, Freeze RA (1983) Chemical hydrogeology: benchmark papers in geology, vol 73. Hutchinson Ross Publication Company, Stroudsburg, p 416
- Capizzi P, Cellura D, Cosentino P, Fiandaca G, Martorana R, Messina P, Schiavone S, Valenza M (2010) Integrated hydrogeochemical and geophysical surveys for a study of seawater intrusion. *Boll Geofis Teor Appl* 51(4):285–300
- Choudhury K, Saha DK, Ghosh DC (2000) Urban geophysical studies on the groundwater environment in parts of Gangetic Delta. *J Geol Soc India* 55:257–267
- Climate Data (2015) Climate: Age Mowo. <http://en.climatedata.org/location/387040>
- Coode Blizzard Ltd., Akute Geo-Resource Ltd., Rofe Kennard, Lapworth (1996) Hydrogeological investigation of Lagos state. Final report, vol I, II
- Cooper HH Jr (1964) A hypothesis concerning the dynamic balance of fresh water and salt water in a coastal aquifer. U.S. geological survey water-supply paper 1613–C, pp 1–12
- Custodio E (1987) Groundwater problems in coastal areas. *Studies and reports in hydrology*. UNESCO, Paris, p 596
- Dey A, Morrison HF (1979) Resistivity modeling for arbitrary shaped two-dimensional structures. *Geophys Prospect* 27:1020–1036
- Egbai JC, Efeyi P (2013) Geoelectric method for investigating salt-water intrusion into freshwater aquifer in Deghele Community of Warri South Local Government Area of Delta State. *Tech J Eng Appl Sci* 3(10):819–827
- Eloisa DS, Viviana R, Nicoletta C, Antonio G (2012) Freshwater–saltwater interactions in the shallow aquifers of Venice lagoon mainland. *Dix-huitiemes journees technique du Comite Francais d'Hydrogeologie de l' Association internationale des hydrogeologues*. Resources of gestion des aquifers lithoraux. Casis, pp 181–188
- Freeze RA, Cherry JA (1979) *Groundwater*, vol 7632. Prentice Hall, New Jersey, p 604
- Goldman M, Kafri U (2004) Hydrogeophysical applications in coastal aquifers. In: Vereecken H, Binley A, Cassiani G, Revil A, Titov K (eds) *Applied hydrogeophysics*. Springer NATO science series IV: earth and environmental science, vol 71. Springer, Berlin, pp 233–254
- Hinrichsen D (2007) Ocean planet in decline. <http://www.peopleandplanet.net/?lid=26188&topic=44§ion=35>. Accessed 7 Nov 2007
- Idowu TE, Nyadawa M, K'Orowe MO (2017) Hydrogeochemical assessment of a coastal aquifer using statistical and geospatial techniques: case study of Mombasa North Coast. *Kenya Environ Earth Sci* 76:422. <https://doi.org/10.1007/s12665-017-6738-y>
- Jones HA, Hockey RD (1964) The geology of part of southwestern Nigeria. *Bull Geol Surv Niger* 31:101–104
- Kampsax-Kruger, Sshwed Associates (1977) Underground water resources of the Metropolitan Lagos. Final Report to Lagos State Ministry of Works, p 170
- Loke MH (2004) Tutorial: 2-D and 3-D electrical imaging surveys, revised edn, p 136. <http://www.geometrics.com/>
- Loke MH, Baker RD (1996) Rapid least squares inversion of apparent resistivity pseudosection using a quasi-Newton method. *Geophys Prospect* 44:131–152

- Nigerian Standard for Drinking Water Quality (NSDQW) (2007) Nigerian Industrial Standard NIS 554, Standard Organization of Nigeria, p 30
- Nton ME (2001) Sedimentological and geochemical studies of rock units in the eastern Dahomey basin, south western Nigeria. Unpublished Ph.D. thesis, University of Ibadan, p 315
- Obaje NG (2009) Geology and mineral resources of Nigeria. Springer, Dordrecht, p 221. <https://doi.org/10.1007/978-3-540-92685-6>
- Okosun EA (1990) A review of the Cretaceous stratigraphy of the Dahomey Embayment, West Africa. *Cretaceous Res* 11:17–27
- Oladapo MI, Ilori OB, Adeoye-Oladapo OO (2014) Geophysical study of saline water intrusion in Lagos municipality. *Afr J Environ Sci Technol* 8(1):16–30. <https://doi.org/10.5897/AJEST2013.1554>
- Omatsola ME, Adegoke OS (1981) Tectonic and cretaceous stratigraphy of the Dahomey basin. *J Geol Min Res* 154(1):65–68
- Oteri AU (1988) Electric log interpretation for the evaluation of saltwater intrusion in the eastern Niger Delta. *Hydrol Sci J* 33(1):19–30. <https://doi.org/10.1080/02626668809491219>
- Oteri AU, Atolagbe FP (2003) Saltwater intrusion into coastal aquifers in Nigeria. In: The second international conference on saltwater intrusion and coastal aquifers: monitoring, modelling and management. Mérida, Yucatán, Mexico, pp 2–4
- Samsudin AR, Baharuddin B, Mustapha M, Soed S (2002) Geophysical mapping of saltwater intrusion in the Kerpan coastal area, Kedah. In: Proceeding of Geological society of Malaysia annual geological conference, Malaysia, pp 135–138
- Silvester PP, Ferrari RL (1996) Finite elements for electrical engineers, 3rd edn. Cambridge University Press, Cambridge, p 494

Publisher's Note Springer Nature remains neutral with regard to jurisdictional claims in published maps and institutional affiliations.